AJNR

Detection of Middle Ear Cholesteatoma by Diffusion-Weighted MR Imaging: Multishot Echo-Planar Imaging Compared with Single-Shot Echo-Planar Imaging

K. Yamashita, T. Yoshiura, A. Hiwatashi, H. Kamano, T. Dashjamts, S. Shibata, A. Tamae and H. Honda

AJNR Am J Neuroradiol 2011, 32 (10) 1915-1918
doi: https://doi.org/10.3174/ajnr.A2651
http://www.ajnr.org/content/32/10/1915

ORIGINAL RESEARCH

Detection of Middle Ear Cholesteatoma by Diffusion-Weighted MR Imaging: Multishot Echo-Planar Imaging Compared with Single-Shot Echo-Planar Imaging

K. Yamashita
T. Yoshiura
A. Hiwatashi
H. Kamano
T. Dashjamts
S. Shibata
A. Tamae
H. Honda

BACKGROUND AND PURPOSE: Previous reports have shown that DWI is useful in detecting cholesteatoma. SS-EPI is the most widely used DWI technique. However, SS-EPI may have susceptibility artifacts due to field inhomogeneity in the imaging of the temporal bone region. Our purpose was to prospectively evaluate the advantage of MS-EPI for the diagnosis of middle ear cholesteatoma by comparing it with SS-EPI.

MATERIALS AND METHODS: We studied 29 patients with preoperatively suspected acquired cholesteatoma. Each patient underwent an MR imaging examination including both SS-EPI and MS-EPI by using a 1.5T MR imaging scanner. Images of the 29 patients (58 temporal bones including 30 with and 28 without cholesteatoma) were reviewed by 2 independent neuroradiologists. The confidence level for the presence of cholesteatoma was graded on a scale of 0–2 (0 = none, 1 = equivocal, 2 = definite). Interobserver agreement as well as sensitivity, specificity, and accuracy were assessed for the 2 readers.

RESULTS: Excellent interobserver agreement was shown for both MS-EPI ($\kappa = 0.856$) and SS-EPI ($\kappa = 0.820$). MS-EPI was associated with higher sensitivity (76.7%) and accuracy (87.9%) than SS-EPI (sensitivity = 50.0%, accuracy = 74.1%) ($P < .05$), while both methods showed 100% specificity.

CONCLUSIONS: Compared with SS-EPI, MS-EPI improves the accuracy of the diagnosis of acquired middle ear cholesteatomas.

ABBREVIATIONS: DWI = diffusion-weighted imaging; MS-EPI = multishot echo-planar imaging; PROPELLER = periodically rotated overlapping parallel lines with enhanced reconstruction; SENSE = sensitivity encoding; SNR = signal-to-noise ratio; SS-EPI = single-shot echo-planar imaging; TSE = turbo spin-echo

While cholesteatoma can often be diagnosed only by otoscopic examination, CT and MR imaging provide cholesteatoma spread and help to grasp anatomic relationships with the middle and inner ear in surgery planning. Since the advent of multidetector row CT, soft-tissue masses and middle and inner ear organs have been clearly depicted by high spatial resolution.[1,2] In contrast, the soft-tissue attenuation can be caused by cholesteatoma, granulation, or fibrous tissue. MR imaging plays an important role in ruling out diseases other than cholesteatoma; and the usefulness of DWI[3-17] and delayed contrast-enhanced imaging[18-20] in diagnosing cholesteatoma has been reported. Compared with delayed contrast-enhanced imaging, DWI is more practical, with a much shorter examination time and no need for contrast injection. On DWI, cholesteatoma shows conspicuous hyperintensity.

In clinical practice, SS-EPI is the most widely used DWI technique because of its rapid data-sampling ability, though it has limited spatial resolution and geometric distortion due to susceptibility artifacts in the imaging of the temporal bone region, which often result in false-negative findings.[4,10-13,16] On the other hand, MS-EPI is known to provide high-resolution DWI with reduced geometric distortions and an SNR similar to that of SS-EPI, at the expense of a longer imaging time.[21-23] However, to our knowledge, its usefulness in the imaging of cholesteatoma has not been established.

Our purpose was to evaluate the advantage of MS-EPI for the diagnosis of middle-ear cholesteatoma by comparing it with SS-EPI.

Materials and Methods

Case Selection

This study was approved by the institutional review board of our hospital. Written informed consent was obtained from all patients. These patients underwent MR imaging between July 2009 and August 2010. We prospectively studied 29 consecutive patients (13 men and 16 women; age range, 18–81 years of age; mean, 49.4 ± 17.2 years) who planned to undergo surgery. One of these patients was suspected of having bilateral primary cholesteatoma, while unilateral disease was suspected in the other 28 patients (18 primary and 10 recurrent). These patients underwent preoperative MR imaging on the day before surgery. Final diagnosis was surgically determined by 2 otorhinolaryngologists, with 12 and 11 years of experience.

Received December 12, 2010; accepted after revision February 17, 2011.

From the Departments of Clinical Radiology (K.Y., T.Y., A.H., H.K., T.D., H.H.) and Otorhinolaryngology (S.S., A.T.), Graduate School of Medical Sciences, Kyushu University, Fukuoka, Japan.

Please address correspondence to Takashi Yoshiura, MD, PhD, Department of Clinical Radiology, Graduate School of Medical Sciences, Kyushu University, 3-1-1 Maidashi, Higashi-ku, Fukuoka 812-8582, Japan; e-mail: tyoshiu@med.kyushu-u.ac.jp

http://dx.doi.org/10.3174/ajnr.A2651

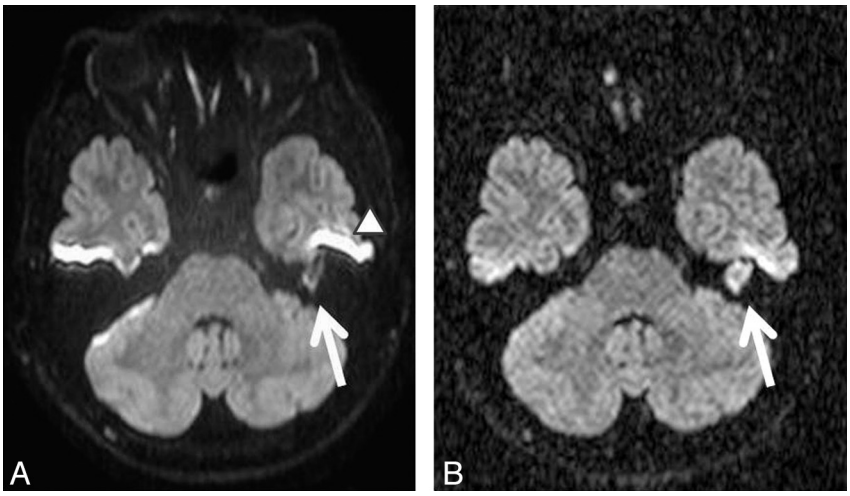

Fig 1. MS-EPI (*B*) compared with SS-EPI (*A*). *A,* Transverse MR images of a cholesteatoma of the left middle ear in a 27-year-old man. SS-EPI shows a slightly hyperintense lesion in the left middle ear (*arrow*). However, the lesion is obscure because of a curvilinear hyperintense area (*arrowhead*) due to field inhomogeneity. *B,* The same lesion is clearly visualized as a marked hyperintensity on MS-EPI.

Imaging Technique

Each patient underwent MR imaging with a 1.5T MR imaging unit (Achieva Nova Dual; Philips Healthcare, Best, the Netherlands) and an 8-channel array head coil. Transverse T2-weighted TSE images (TR/TE, 2720/110 ms; 90° flip angle; NEX, 8; SENSE factor, 2; 12 sections; section thickness/gap, 2/1 mm; 170-mm FOV; 240 × 180 matrix; imaging time, 3 minutes 40 seconds) and transverse T1-weighted TSE images (TR/TE, 472/18 ms; 75° flip angle; NEX, 4; 12 sections; section thickness/gap, 2/1 mm; 170-mm FOV; 240 × 180 matrix; imaging time, 3 minutes 56 seconds) were obtained. In addition, transverse SS-EPI (TR/TE, 3000/59 ms; 90° flip angle, NEX, 4; b factor, 1000 s/mm^2; SENSE factor, 2.5; section thickness/gap, 2/1 mm; 230-mm FOV; 128 × 256 matrix; imaging time, 1 minute 30 seconds) and MS-EPI (TR/TE, 2250–3000/76 ms; 90° flip angle; NEX, 3; number of shots, 4; b factor, 800 s/mm^2; section thickness/gap, 2/1 mm; 230-mm FOV; 128 × 256 matrix; imaging time, 4 minutes 21 seconds) were also obtained (Fig 1). For MS-EPI, a trigger delay of 250 ms after the peripheral pulse wave was chosen to reduce motion artifacts.[24,25]

Image Evaluation

Images of the patients were reviewed by 2 independent neuroradiologists (with 9 and 7 years of experience) who were blinded to the patients' clinical information. The confidence level for the presence of cholesteatoma was graded on a scale of 0–2 (0 = none, 1 = equivocal, 2 = definite). The 2 radiologists assessed T1-weighted images, T2-weighted images, and MS-EPI or SS-EPI. T2-weighted images were used as anatomic references. The image sets with SS-EPI and those with MS-EPI were mixed and presented to the observer in a random order. The definite presence of cholesteatoma (score 2) was diagnosed when marked hyperintensity compared with the brain tissue was noted on DWI, unless the same lesion showed hyperintensity compared with the cerebral white matter on T1-weighted images, which strongly suggested cholesterol granuloma.[15,26] When the hyperintensity of the lesions on DWI was not marked or the DWI hyperintensity coexisted with hyperintensity on T1-weighted images, the lesion was rated a 1 on the confidence level scale. In all other cases, the lesions were rated zero. Only a score of 2 was defined as a positive result.

Sensitivity, specificity, and accuracy for the detection of cholesteatoma with SS-EPI and MS-EPI[a]

	Sensitivity (%)[b]	Specificity (%)	Accuracy (%)[b]
Observer 1			
SS-EPI	46.7 (14/30)	100 (28/28)	72.4 (42/58)
MS-EPI	76.7 (23/30)	100 (28/28)	87.9 (51/58)
Observer 2			
SS-EPI	46.7 (14/30)	100 (28/28)	75.9 (44/58)
MS-EPI	76.7 (23/30)	100 (28/28)	87.9 (51/58)

[a] Numbers in parentheses are raw data.
[b] $P < .05$ (Pearson χ^2 test).

Statistical Analysis

The interobserver agreement on the rating scale was evaluated by using the κ statistic based on the published literature.[27] In addition, the sensitivity, specificity, and accuracy of the detection of cholesteatoma were compared between MS-EPI and SS-EPI by using the Pearson χ^2 test. Multiple logistic regression analysis between the 2 methods was used to identify the contributing factors. Statistical analyses were performed by using PASW Statistics 18 (SPSS, Chicago, Illinois). In all statistical analyses, the level of significance was set at $P < .05$.

Results

The diagnosis of cholesteatoma was surgically confirmed in all patients who were clinically suspected of having cholesteatoma. Because 1 patient had bilateral cholesteatoma and 1 patient had no cholesteatoma, a total of 30 temporal bones with cholesteatomas (20 primary and 10 recurrent) and 28 without were assessed by the observers.

Excellent interobserver agreement was found for both MS-EPI ($\kappa = 0.856$) and SS-EPI ($\kappa = 0.820$). MS-EPI was associated with a higher sensitivity (76.7%) and accuracy (87.9%) than SS-EPI (sensitivity = 50.0%, accuracy = 74.1%) ($P < .05$), while both methods showed 100% specificity (Table).

There were 16 and 14 false-negative cases on SS-EPI for observers 1 and 2, respectively; those on MS-EPI were 7 and 7 for observers 1 and 2, respectively. Four cholesteatomas were undetectable on both SS-EPI and MS-EPI. These lesions were also undetectable on both T1- and T2-weighted images, even on retrospective observation (Fig 2).

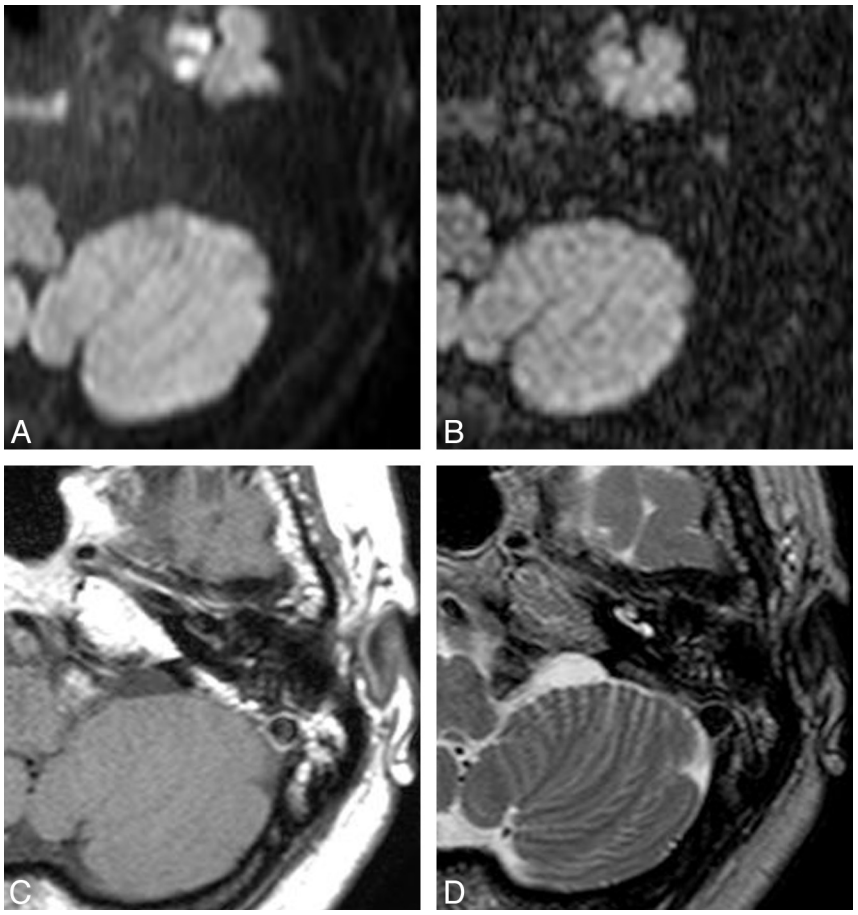

Fig 2. MR images of a recurrent cholesteatoma of the left middle ear in a 42-year-old woman. Cholesteatoma is undetectable not only on SS-EPI (*A*) and MS-EPI (*B*) but also on T1- (*C*) and T2-weighted images (*D*), even on retrospective observation. A very small cholesteatoma was found along the columella formed by the incus during the surgery.

Multiple logistic regression analysis showed that MS-EPI was the only independent discriminator to predict cholesteatoma ($P < .001$).

Discussion

Our results showed that MS-EPI showed increased diagnostic accuracy for acquired cholesteatoma compared with the conventional SS-EPI technique (Table).

The usefulness of DWI in the detection of cholesteatoma has been described in many published reports.[3-17] DWI reflects altered water molecular mobility. It is postulated that restricted free water molecular diffusion, T2 "shine through" effect, or a combination of both was responsible for the marked hyperintensity on DWI.[15,28,29] Recently, De Foer et al[17] reported that DWI sequences had significantly higher sensitivity and specificity than delayed gadolinium-enhanced T1-weighted sequences.

SS-EPI requires only a single radio-frequency excitation pulse, and it is the most widely used DWI technique in clinical practice.[11,20,30] SS-EPI is known to be very susceptible to main field inhomogeneity, which may lead to severe image degradation. In MS-EPI, signal-intensity acquisition can be divided into a number of shots with interleaved *k*-space trajectories, which result in reduced imaging distortion[25] and a similar SNR compared with SS-EPI.[21-23] We believe that the better sensitivity and accuracy of MS-EPI compared with SS-EPI shown in this study is attributable to the improved image quality of the former. MS-EPI in this study required a longer examination time (4 minutes 21 seconds) than SS-EPI (1 minute 30 seconds). Nevertheless, our results suggest that the increased value of MS-EPI more than offsets the increased expense of the longer imaging time.

Although non-echo-planar imaging techniques such as PROPELLER have been reported to be useful in avoiding geometric distortion in DWI due to nonuniform signal-intensity averages in different portions of the *k*-space,[6] the signal-intensity characteristics were more favorable with echo-planar imaging than with PROPELLER.[31] In addition, PROPELLER is unavailable in most MR imaging systems including our system, while MS-EPI requires no special installation and is, therefore, widely available. A comparison of image quality between DWI obtained by using the non-echo-planar imaging techniques and that obtained with MS-EPI should be studied in the future.

Four cholesteatomas could not be detected on either MS-EPI or SS-EPI in this study. These lesions were undetectable not only on DWI but also on T1- and T2-weighted images, even on retrospective observation (Fig 2). In each of these 4 cases, a thin membrane-like or very small cholesteatoma lesion was found during the surgery. Fitzek et al[30] presumed that a false-negative on imaging might occur in cases of very early cholesteatoma without mass formation or when cholesteatoma masses spontaneously extruded into the external auditory canal before MR imaging.

This study has several limitations. First, the number of patients was relatively limited. Second, the apparent diffusion coefficient was not evaluated to confirm decreased diffusion, and contrast-enhanced T1-weighted imaging was not evaluated. We focused on evaluating the 2 echo-planar methods, and MS-EPI showed positive results in this study. Third, different TEs were selected for MS-EPI (76 ms) and SS-EPI (59 ms). We chose the minimum TE to maximize the SNR for each pulse sequence. Finally, we used different b factors for the 2 sequences: 800 s/mm^2 for MS-EPI and 1000 seconds/mm^2 for SS-EPI. Although the optimum b factor has not yet been determined for the head and neck region, b factors between 800 and 1000 s/mm^2 have been most commonly used.[3-20] Although we should have used the same b factors for the 2 imaging methods, we believe that the effect of the different b factors distorted our results only minimally. Kingsley and Monahan[32] noted that the exact choice of b factor is not critical for the detection of ischemic strokes when a b factor between 800 and 1200 s/mm^2 is used.

Conclusions

Our results demonstrate that MS-EPI improves the diagnostic accuracy for acquired middle ear cholesteatomas in comparison with SS-EPI. The use of MS-EPI instead of SS-EPI should be considered as a clinical imaging protocol for cholesteatoma.

Acknowledgments

We thank Shutaro Saiki for providing his valuable expertise on setup MR imaging parameters for this article.

References

1. Marchioni D, Mattioli F, Cobelli M, et al. **CT morphological evaluation of anterior epitympanic recess in patients with attic cholesteatoma.** *Eur Arch Otorhinolaryngol* 2009;266:1183–89
2. Park MH, Rah YC, Kim YH, et al. **Usefulness of computed tomography Hounsfield unit density in preoperative detection of cholesteatoma in mastoid ad antrum.** *Am J Otolaryngol* 2011;32:194–97. Epub 2010 Apr 30
3. Cimsit NC, Cimsit C, Baysal B, et al. **Diffusion-weighted MR imaging in postoperative follow-up: reliability for detection of recurrent cholesteatoma.** *Eur J Radiol* 2010;74:121–23
4. De Foer B, Vercruysse JP, Pilet B, et al. **Single-shot, turbo spin-echo, diffusion-weighted imaging versus spin-echo-planar, diffusion-weighted imaging in the detection of acquired middle ear cholesteatoma.** *AJNR Am J Neuroradiol* 2006;27:1480–82
5. Maheshwari S, Mukherji SK. **Diffusion-weighted imaging for differentiating recurrent cholesteatoma from granulation tissue after mastoidectomy: case report.** *AJNR Am J Neuroradiol* 2002;23:847–49
6. Lehmann P, Saliou G, Brochart C, et al. **3T MR imaging of postoperative recurrent middle ear cholesteatomas: value of periodically rotated overlapping parallel lines with enhanced reconstruction diffusion-weighted MR imaging.** *AJNR Am J Neuroradiol* 2009;30:423–27
7. Thiriat S, Riehm S, Kremer S, et al. **Apparent diffusion coefficient values of middle ear cholesteatoma differ from abscess and cholesteatoma admixed infection.** *AJNR Am J Neuroradiol* 2009;30:1123–26
8. Aikele P, Kittner T, Offergeld C, et al. **Diffusion-weighted MR imaging of cholesteatoma in pediatric and adult patients who have undergone middle ear surgery.** *AJR Am J Roentgenol* 200;181:261–65
9. Vercruysse JP, De Foer B, Pouillon M, et al. **The value of diffusion-weighted MR imaging in the diagnosis of primary acquired and residual cholesteatoma: a surgical verified study of 100 patients.** *Eur Radiol* 2006;16:1461–67
10. De Foer B, Vercruysse JP, Bernaerts A, et al. **The value of single-shot turbo spin echo diffusion-weighted MR imaging in the detection of middle ear cholesteatoma.** *Neuroradiology* 2007;49:841–48
11. Stasolla A, Magliulo G, Parrotto D, et al. **Detection of postoperative relapsing/residual cholesteatomas with diffusion-weighted echo-planar magnetic resonance imaging.** *Otol Neurotol* 2004;25:879–84
12. De Foer B, Vercruysse JP, Bernaerts A, et al. **Detection of postoperative residual cholesteatoma with non-echo-planar diffusion weighted magnetic resonance imaging.** *Otol Neurotol* 2008;29:513–17
13. Dhepnorrarat RC, Wood B, Rajan GP. **Postoperative non-echo-planar diffusion weighted magnetic resonance imaging changes after cholesteatoma surgery: implications or cholesteatoma screening.** *Otol Neurotol* 2009;30:54–58
14. Jeunen G, Desloovere C, Hermans R, et al. **The value of magnetic resonance imaging in the diagnosis of residual or recurrent acquired cholesteatoma after canal wall-up tympanoplasty.** *Otol Neurotol* 2008;29:16–18
15. Dubrulle F, Souillard R, Chechin D, et al. **Diffusion-weighted MR imaging sequence in the detection of postoperative recurrent cholesteatoma.** *Radiology* 2006;238:604–10
16. Schwartz KM, Lane JI, Bolster BD Jr, et al. **The utility of diffusion-weighted imaging for cholesteatoma evaluation.** *AJNR Am J Neuroradiol* 2011;32:430–36. Epub 2010 May 20
17. De Foer B, Vercruysse JP, Bernaerts A, et al. **Middle ear cholesteatoma: non-echo-planar diffusion-weighted MR imaging versus delayed gadolinium-enhanced T1-weighted MR imaging—value in detection.** *Radiology* 2010;255:866–72
18. Williams MT, Ayache D, Alberti C, et al. **Detection of postoperative residual cholesteatoma with delayed contrast-enhanced MR imaging: initial findings.** *Eur Radiol* 200;13:169–74
19. Ayache D, Williams MT, Lejeune D, et al. **Usefulness of delayed postcontrast magnetic resonance imaging in the detection of residual cholesteatoma after canal wall-up tympanoplasty.** *Laryngoscope* 2005;115:607–10
20. Venail F, Bonafe A, Poirrier V, et al. **Comparison of echo-planar diffusion weighted imaging and delayed postcontrast T1-weighted MR imaging for the detection of residual cholesteatoma.** *AJNR Am J Neuroradiol* 2008;29:1363–68
21. Skare S, Newbould RD, Clayton DB, et al. **Clinical multishot DW-EPI through parallel imaging with considerations of susceptibility, motion, and noise.** *Magn Reson Med* 2007;57:881–90
22. Nana R, Zhao T, Hu X. **Single-shot multiecho parallel echo-planar imaging (EPI) for diffusion tensor imaging (DTI) with improved signal-to-noise ratio (SNR) and reduced distortion.** *Magn Reson Med* 2008;60:1512–17
23. Hennel F. **Image-based reduction of artifacts in multishot echo-planar imaging.** *J Magn Reson* 1998;134:206–13
24. Skare S, Andersson JL. **On the effects of gating in diffusion imaging of the brain using single shot EPI.** *Magn Reson Imaging* 2001;19:1125–28
25. Bammer R. **Basic principles of diffusion-weighted imaging.** *Eur J Radiol* 2003;45:169–84
26. Kösling S, Bootz F. **CT and MR imaging after middle ear surgery.** *Eur J Radiol* 2001;40:113–18
27. Sim J, Wright CC. **The kappa statistic in reliability studies: use, interpretation, and sample size requirements.** *Phys Ther* 2005;85:257–68
28. Annet L, Duprez T, Grandin C, et al. **Apparent diffusion coefficient measurements within intracranial epidermoid cysts in six patients.** *Neuroradiology* 2002;44:326–28
29. Schaefer PW, Grant PE, Gonzalez RG. **Diffusion-weighted MR imaging of the brain.** *Radiology* 2000;217:331–45
30. Fitzek C, Mewes T, Fitzek S, et al. **Diffusion-weighted MRI of cholesteatomas of the petrous bone.** *J Magn Reson Imaging* 2002;15:636–41
31. Abe O, Mori H, Aoki S, et al. **Periodically rotated overlapping parallel lines with enhanced reconstruction-based diffusion tensor imaging: comparison with echo planar imaging-based diffusion tensor imaging.** *J Comput Assist Tomogr* 2004;28:654–60
32. Kingsley PB, Monahan WG. **Selection of the optimum b factor for diffusion-weighted magnetic resonance imaging assessment of ischemic stroke.** *Magn Reson Med* 2004;51:996–1001